The Plant Cell, Vol. 11, 1995–2011, October 1999, www.plantcell.org © 1999 American Society of Plant Physiologists

Glutamine Synthetase in the Phloem Plays a Major Role in Controlling Proline Production

Norbert Brugière,[a,1] Frédéric Dubois,[b] Anis M. Limami,[a] Maud Lelandais,[a] Yvette Roux,[a] Rajbir S. Sangwan,[b] and Bertrand Hirel[a,2]

[a] Laboratoire du Métabolisme et de la Nutrition des Plantes, INRA de Versailles, Route de St. Cyr, F-78026 Versailles Cedex, France
[b] Laboratoire d'Androgénèse et Biotechnologie, Université de Picardie Jules Verne, 33 rue Saint-Leu, Ilot des Poulies, F-80039 Amiens Cedex, France

To inhibit expression specifically in the phloem, a 274-bp fragment of a cDNA (*Gln1-5*) encoding cytosolic glutamine synthetase (GS1) from tobacco was placed in the antisense orientation downstream of the cytosolic Cu/Zn superoxide dismutase promoter of *Nicotiana plumbaginifolia.* After Agrobacterium-mediated transformation, two transgenic *N. tabacum* lines exhibiting reduced levels of *GS1* mRNA and GS activity in midribs, stems, and roots were obtained. Immunogold labeling experiments allowed us to verify that the GS protein content was markedly decreased in the phloem companion cells of transformed plants. Moreover, a general decrease in proline content in the transgenic plants in comparison with wild-type tobacco was observed when plants were forced to assimilate large amounts of ammonium. In contrast, no major changes in the concentration of amino acids used for nitrogen transport were apparent. A $^{15}NH_4^+$-labeling kinetic over a 48-hr period confirmed that in leaves of transgenic plants, the decrease in proline production was directly related to glutamine availability. After 2 weeks of salt treatment, the transgenic plants had a pronounced stress phenotype, consisting of wilting and bleaching in the older leaves. We conclude that GS in the phloem plays a major role in regulating proline production consistent with the function of proline as a nitrogen source and as a key metabolite synthesized in response to water stress.

INTRODUCTION

In higher plants, glutamine synthetase (GS; EC 6.3.1.2) is a key enzyme involved in the assimilation of inorganic nitrogen into organic forms (O'Neal and Joy, 1973; Lea and Miflin, 1974). GS catalyzes the ATP-dependent condensation of ammonium with glutamate to yield glutamine, which then provides nitrogen groups, either directly or via glutamate for the biosynthesis of all nitrogenous compounds in the plant (Lea et al., 1989).

Two groups of GS isoenzymes, plastidic (GS2) and cytosolic (GS1), have been identified in higher plants (McNally et al., 1983; Hirel et al., 1993). In the majority of higher plants, GS2 is predominant in most chlorophyllous tissue and is localized in the chloroplast stroma (Botella et al., 1988; Brangeon et al., 1989; Dubois et al., 1996). In a limited number of species, such as legumes, GS2 was shown to be present also in plastids of either roots (Vézina and Langlois, 1989) or root nodules (Lightfoot et al., 1988; Brangeon et al., 1989), representing ~5% of total GS protein content. More recently, isolation of cDNAs encoding GS2 allowed the demonstration that in most plant species, this isoenzyme is encoded by a single nuclear gene per haploid genome (Lightfoot et al., 1988; Becker et al., 1992). Using photorespiratory mutants of barley that were deficient in leaf GS2 activity, Blackwell et al. (1987) and Wallsgrove et al. (1987) demonstrated that GS2 is indispensable for the reassimilation of ammonium released from the photorespiratory nitrogen cycle. Interestingly, these mutants possess levels of GS1 protein and activity comparable to the wild type and display no phenotypic changes when grown under nonphotorespiratory conditions (Blackwell et al., 1987; Wallsgrove et al., 1987). Therefore, these observations imply that root and leaf GS1 activities that remain in these mutants are sufficient for normal plant growth and development.

GS1 is predominant in roots (Hirel et al., 1993; Oliveira et al., 1997). However, in shoots, its activity relative to GS2 varies between tissues and between species examined (McNally and Hirel, 1983; McNally et al., 1983). Immunocytochemical evidence has demonstrated that leaf GS1 protein is localized in the vascular tissue, in which a high proportion of the protein is concentrated in the phloem companion cells (Carvalho et al., 1992; Kamachi et al., 1992; Pereira et al., 1992; Dubois et al., 1996; Peat and Tobin, 1996; Sakurai et

[1] Current address: Department of Molecular Biology and Genetics, College of Biological Science, University of Guelph, Guelph, Ontario N1G 2W1, Canada.
[2] To whom correspondence should be addressed. E-mail hirel@versailles.inra.fr; fax 33-1-30-83-30-96.

al., 1996). However, in C_4 plants, such as maize, additional GS1 protein and activity have been detected in the cytosol of both bundle sheath and mesophyll cells (Yamaya and Oaks, 1988; Becker et al., 1993).

The physiological role of leaf GS1 remains to be elucidated. In most species examined thus far, GS1 is encoded by a multigene family composed of at least three different members (Cullimore et al., 1984; Gebhardt et al., 1986; Tingey et al., 1987, 1988; Lightfoot et al., 1988; Peterman and Goodman, 1991; Li et al., 1993; Roche et al., 1993; Lam et al., 1995). In tobacco, two of these, *Gln1-5* and *Gln1-3*, have been characterized previously, and the corresponding cDNAs were used to study transcript abundance in vegetative and reproductive organs (Dubois et al., 1996). We showed that *Gln1-5* transcripts are expressed mainly in the phloem, whereas *Gln1-3* transcripts are abundant in the cytosol of roots and floral organs, such as petals, anthers, and ovaries (Dubois et al., 1996). Although it is generally thought that GS1 plays a major role in the assimilation of ammonium derived from nitrate reduction in roots, the role of GS1 in the vascular tissue is not well defined. One possibility is that GS1 may be involved in vascular nitrogen transport (Edwards et al., 1990; Dubois et al., 1996). Interestingly, induction of GS1 has been observed in tissues such as senescing leaves and cotyledons (Kawakami and Watanabe, 1988; Kamachi et al., 1991; Bernhard and Matile, 1994; Watanabe et al., 1994; Pérez-Rodríguez and Valpusta, 1996), suggesting that GS1 also may be involved in the remobilization of nitrogen. Consistent with this hypothesis, *Lotus corniculatus* plants overexpressing GS1 in the leaf cytosol exhibited accelerated nitrogen remobilization (Vincent et al., 1997).

To date, no GS1 mutants have been isolated, possibly because there is more than one gene encoding GS1 and each is differentially expressed in a particular organ or tissue. Therefore, we decided to develop an RNA antisense strategy to decrease or eliminate the expression of single members of the GS1 multigene family. To investigate the role of GS1 in vascular tissue, inhibition of the expression of GS1 specifically in the phloem was achieved using tobacco as a model system (Dubois et al., 1996). Molecular and immunocytochemical analyses were performed to select transgenic *Nicotiana tabacum* plants with reduced GS activity in the phloem. Measurement of various parameters, such as amino acid and ammonium content in leaves roots and phloem sap, was used to evaluate the physiological impact of modified GS activity.

RESULTS

Phloem-Specific Expression of an Antisense Cystolic *GS* Gene Results in a Decrease in GS1 Protein and Activity in the Vascular Tissue of Transgenic Tobacco Plants

A 274-bp fragment from the coding region of the tobacco *Gln1-5* cDNA, which corresponds to a *GS* gene specifically expressed in the phloem (Dubois et al., 1996; EMBL accession number X95932), was placed in the antisense orientation downstream of the cytosolic Cu/Zn superoxide dismutase (*SOD*) promoter of *N. plumbaginifolia* (Hérouart et al., 1993). This promoter directs phloem-specific expression of a β-glucuronidase reporter gene in transgenic tobacco plants (Hérouart et al., 1994). The construct was cloned into a pBI-type vector (Bevan, 1984) and introduced in tobacco via Agrobacterium-mediated transformation using a leaf disc protocol (Horsch et al., 1985). Kanamycin-resistant tobacco plants were regenerated, and eight independent primary transformants were selected for further analysis. The steady state level of *GS1* mRNA in midribs of transgenic tobacco plants was determined by RNA gel blot analysis using the ^{32}P-labeled insert of *Gln1-5* cDNA (Dubois et al., 1996) as a probe. Because it does not cross-hybridize with *GS2* mRNA, the *Gln1-5* probe allows quantitative estimation of the *GS1* transcript amounts (Dubois et al., 1996).

Compared with the untransformed control plants, similar amounts of *GS1* transcripts were detectable in six of the eight independent primary transformants (Figure 1A). *GS1* transcripts were almost undetectable in two primary transformants (Figure 1A, lanes 7 and 9). These two primary transformants were named SOD-AS7 and SOD-AS9. The lower migrating band exhibiting variable intensities corresponds to the *Gln1-5* antisense mRNA present in the different transformants. Interestingly, *Gln1-5* antisense transcripts were absent in three primary transformants, including the SOD-AS7 and SOD-AS9 plants (Figure 1A). Equal amounts of total RNA were loaded in each lane (Figure 1B). In leaf lamina, the concentration of transcripts encoding GS2, which were used as controls to check the specificity of *GS1* mRNA antisense inhibition, remained constant in SOD-AS7 and SOD-AS9 (Figure 1C). SOD-AS7 and SOD-AS9 transformants were selected and self-pollinated. The T_1 progeny were used for further molecular and physiological analyses.

To demonstrate that the observed decrease in *GS1* mRNA corresponded to a relative decrease in the steady state amount of *Gln1-5* mRNA in the leaf midrib, an RNase protection analysis was performed by using a ^{32}P-labeled antisense RNA probe, *NT5*, corresponding to the 3′ untranslated region of *Gln1-5* (Dubois et al., 1996). The mRNA corresponding to *Gln1-5*, represented by a single protected fragment, was not present in SOD-AS7 and SOD-AS9 T_1 transformants (Figure 2A), demonstrating that *Gln1-5* mRNA was absent from their midribs.

In a previous study, we showed that the GS1 isoform encoded by *Gln1-5* was expressed almost exclusively in the vascular tissue (Dubois et al., 1996). Therefore, an RNase protection assay was performed to determine whether *Gln1-5* expression was impaired in stem and root tissues of SOD-AS7 and SOD-AS9 T_1 transformants. *Gln1-5* transcripts were absent from both roots and stems of transgenic plants (Figures 2B and 2C), suggesting that *Gln1-5* mRNA was eliminated in all vegetative organs of tobacco. To check the specificity of the inhibition of *Gln1-5* expression in the

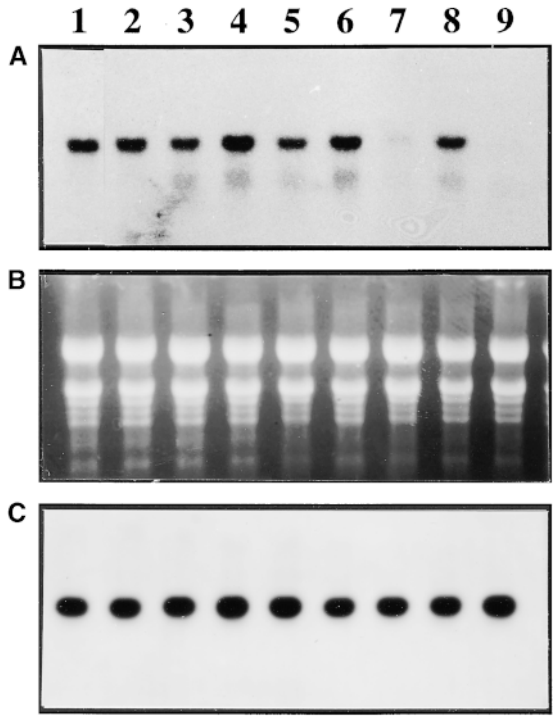

Figure 1. Analysis of *GS* Transcripts in the Midribs and the Leaf Lamina of Primary SOD-AS Tobacco Transformants.

(A) RNA gel blot analysis of the *GS1* mRNA steady state levels in midribs of an untransformed control plant (lane 1) and eight primary transformants containing the *pBI-SOD-AS* construct (lanes 2 to 9). Total RNA samples (10 μg) were hybridized with the tobacco GS cDNA clone *Gln1-5* (Dubois et al., 1996).

(B) The ribosomal RNA bands visible after staining with ethidium bromide.

(C) RNA gel blot analysis of the *GS2* mRNA steady state levels in leaf lamina of an untransformed control plant (lane 1) and eight primary transformants containing *pBI-SOD-AS* (lanes 2 to 9). The total RNA sample (10 μg) was hybridized with the tobacco GS cDNA clone *pGS217* (Becker et al., 1992).

phloem, an additional RNase protection experiment was performed using the ^{32}P-labeled antisense probe *NT3*, which corresponds to the 3′ noncoding region of *Gln1-3* cDNA (Dubois et al., 1996). We have shown previously that *Gln1-3* mRNAs were highly expressed in roots but could not be detected in stems or leaf lamina (Dubois et al., 1996). The results of the RNase protection experiment presented in Figure 2D clearly demonstrate that the expression of *Gln1-3* was not modified in roots of SOD-AS7 and SOD-AS9 T_1 transformants.

To determine whether the decrease in *Gln1-5* gene expression led to a decrease of GS activity, total enzyme activity was measured in crude extracts from roots, stems, and leaf lamina of T_1 SOD-AS7 and SOD-AS9 transformants (Table 1). A 20% decrease in total GS activity was detected in stems of transgenic plants in comparison with untransformed control plants. Similar results were obtained in midribs (data not shown). In roots, a significant decrease of ~30% in total enzyme activity was observed, whereas in leaf lamina, no major changes were detected (Table 1). This result shows that total GS activity was significantly lower only in plant organs containing large amounts of vascular tissue.

The GS isoenzyme content in SOD-AS7 and SOD-AS9 T_1 transformants exhibiting 20% less GS activity in stems was examined after DEAE-Sephacel chromatography (Figure 3). The disappearance of both GS1 protein and GS1 activity (Figures 3A, 3C, and 3D) was observed in transgenic plants containing the GS antisense construct. Analysis of the subunit composition of GS showed that a major polypeptide of 45 kD predominated in stems of both transgenic and untransformed control plants. This polypeptide corresponds to GS2, the plastidic isoform of GS (Figures 3B, 3C, and 3D, fractions 21 to 28). In this tissue, two less abundant polypeptides, namely, α and β, were also identified (38 and 40 kD, respectively). These two smaller peptides are the major components of the GS1 isoform in the phloem of untransformed plants (Figure 3B, fractions 30 to 38) and are almost undetectable in transgenic plants (Figures 3C and 3D, fractions 30 to 38). Whether these two polypeptides correspond to the translation products of two closely related genes encoding *Gln1-5* genes in the amphidiploid genome of *N. tabacum* or are the result of post-translational modifications of a single gene product remains to be determined. Another GS1 subunit (38 kD) also was detected in both transformed and untransformed control plants (Figures 3B to 3D, fractions 21 to 26). However, using our experimental procedures, it was not possible to verify whether this GS1 protein was still active in the stem tissue. Similar results were obtained when leaf midrib protein extracts of SOD-AS7 or SOD-AS9 transgenic plants were submitted to ion exchange chromatography (data not shown).

In root tissue of untransformed control plants, a major polypeptide of 38 kD and a minor polypeptide of 40 kD correspond to the cytosolic form of GS. The polypeptide of 45 kD corresponds to the plastidic form of the enzyme (Figure 3E). In transgenic plants, the 40-kD α polypeptide was undetectable, whereas a 5 to 10% decrease of the 38-kD polypeptide was observed after protein gel blot analysis. This decrease is likely to correspond to the absence of polypeptide β, which also exhibits a molecular mass of 38 kD. The remaining 38-kD polypeptide corresponds to the GS protein present in the roots that was not affected by the antisense inhibition in the vascular tissue (the latter was verified by densitometric scanning of the protein gel blot). Because the α and β polypeptides were present in rather small quantities, it was not possible to confirm by two-dimensional gel electrophoresis whether they were lacking in roots of transgenic plants. After densitometric scanning, no significant differences could be detected in the levels of GS2

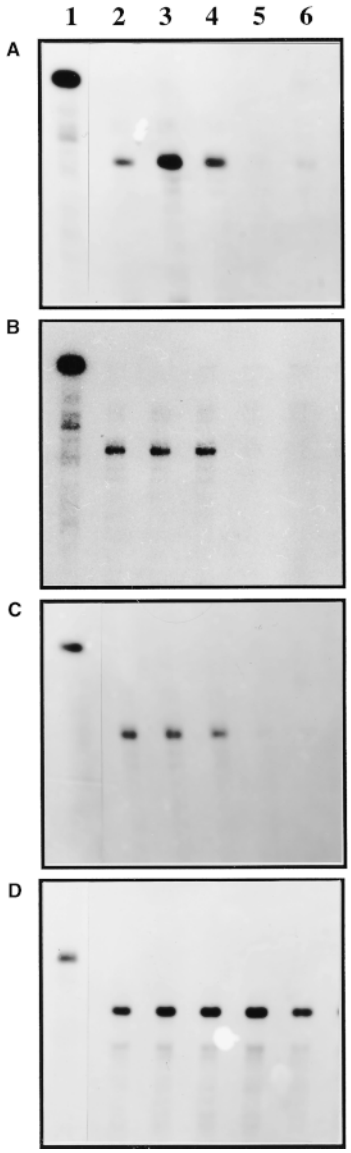

Figure 2. Expression of *GS* Transcripts in Midribs, Stems, and Roots of Untransformed Control Plants and *pBI-SOD-AS* Tobacco T_1 Transformants.

(A) to **(C)** Steady state amount of *Gln1-5* transcripts in midribs **(A)**, stems **(B)**, and roots **(C)** of three different untransformed control plants (lanes 2 to 4) and of the SOD-AS7 and SOD-AS9 T_1 transgenic lines (lanes 5 and 6). S1 nuclease analyses were performed using 10 μg of total RNA. Lanes 1 show the position of the *Gln1-5* antisense probe (243 bp). The length of the probe protected from S1 nuclease digestion in RNA-RNA hybrids is 218 bp.

(D) Steady state amount of *Gln1-3* transcripts in roots of untransformed control plants (lanes 2 to 4) and of the SOD-AS7 and SOD-AS9 T_1 transgenic lines (lanes 5 and 6). Lane 1 shows the position of the *Gln1-3* antisense probe (298 bp). The length of the probe protected from S1 nuclease digestion in RNA-RNA hybrids is 289 bp.

found in roots of transformed and untransformed plants (Figure 3E). Because the GS1 isoenzyme in the root vascular tissue eluted at the same ionic strength as did that of the remainder of the root tissue, it was not possible, as it was with stems or midribs, to separate the two GS1 activities by DEAE-Sephacel chromatography. Moreover, it was not possible to separate GS1 and GS2 activities by using the same technique or affinity chromatography. However, the protein gel blot presented in Figure 3E clearly shows that the amount of GS2 polypetide was similar in both transgenic and untransformed control plants, indicating that the expression of the GS2 isoenzyme was not modified in the antisense plants.

Immunocytochemical studies using both light (Figure 4) and electron microscopy (Figures 5 and 6) techniques were employed to determine at the cellular and intracellular levels whether GS was specifically impaired in the phloem of transformed tobacco plants. GS was localized in stem sections of SOD-AS–transformed tobacco plants and untransformed control plants by using immunogold labeling, followed by silver enhancement (Dubois et al., 1996). Tissue sections treated with gold-labeled anti-GS antibodies recognizing both GS1 and GS2 allowed the detection of GS in the cytosol or the plastids. A bright-field microscope emitting epipolarized light was used for these experiments, and the silver-enhanced gold particles appeared as a bright blue-green color.

The absence of detectable signal in the vascular bundles of sections treated with preimmune serum indicated that there was no unspecific labeling (Figure 4B). Figure 4A gives an overall view of a stem section treated with Periodic Acid Schiff's–Naphtol Blue-Black (PAS-NBB) in which polysaccharides, cell wall, and starch were stained red, with soluble proteins appearing as blue-black.

A stem section of untransformed control plants showed gold particles associated with chloroplasts of the subepidermic cell layer and the amyloplasts of the internal starch sheath layer (Figure 4C), whereas in the vascular bundles, labeling was only detected in the cytoplasm (Figures 4C and 4D). In a similar stem section of SOD-AS transgenic plants,

Table 1. Total GS Activity in SOD-AS–Transformed Plants

	GS Activity (nmol GHA mg protein^{-1} min^{-1})[a]		
Plants	Leaf Lamina	Stems	Roots
Control	122.4 ± 27	40.0 ± 2.1	30.4 ± 2.9
SOD-AS7	122.6 ± 11	32.8 ± 2.5	14.4 ± 6.9
SOD-AS9	131.6 ± 15	31.1 ± 3.1	13.4 ± 4.1

[a] GS activity (GHA) was measured in leaf lamina, stems, and roots of tobacco plants grown for 8 weeks on a complete N12 solution (see Methods). Values are the mean ±SD of six untransformed control plants and the mean of three individual plants of the SOD-AS7 or SOD-AS9 transgenic T_1 lines.

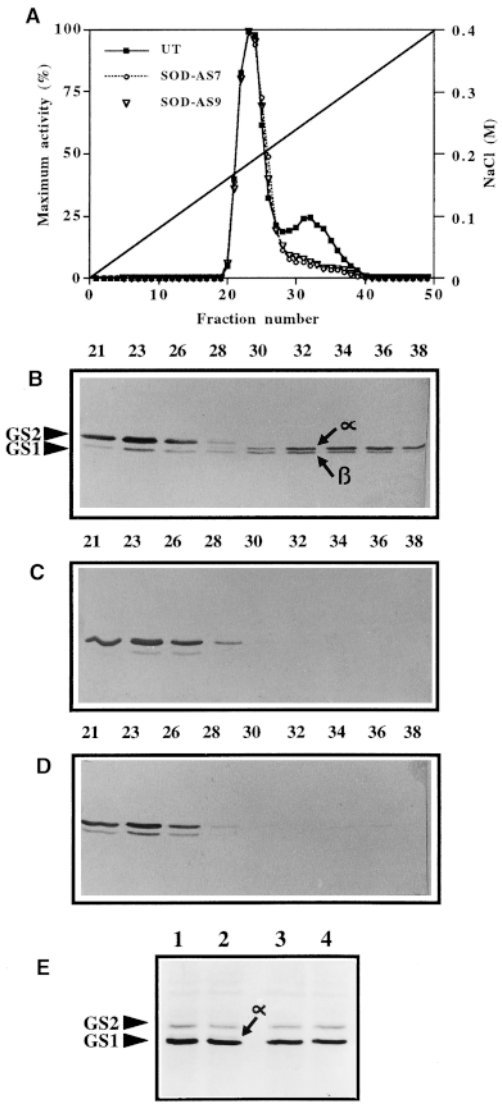

Figure 3. GS Isoenzymes and GS Subunit Composition in SOD-AS–Transformed Plants and Untransformed Control Plants.

(A) DEAE-Sephacel chromatography of GS activity in stem extracts from untransformed (UT) and transformed tobacco SOD-AS7 and SOD-AS9 plants expressing a *GS* antisense mRNA in the phloem. Maximum GS activity was 16 μmol hr^{-1} g^{-1} fresh weight of tissue.

(B) to **(D)** Protein gel analysis of the corresponding peaks of GS activity from fractions 21 to 38 in untransformed **(B)**, SOD-AS7–transformed **(C)**, and SOD-AS9–transformed **(D)** plants. The upper band (molecular mass of 45 kD) corresponds to the GS2 subunits, and the lower bands (molecular mass of 40 kD for polypeptide α and 38 kD for polypeptide β) correspond to the GS1 subunits.

(E) Protein gel blot analysis of GS subunit composition in roots of untransformed (lanes 1 and 2) and SOD-AS7– and SOD-AS9–transformed (lanes 3 and 4) plants. The upper band (molecular mass of 45 kD) corresponds to the GS2 subunits, and the lower bands (molecular masses of 40 and 38 kD) correspond to the GS1 subunits. Polypeptide α corresponds to the phloem-specific GS subunit.

immunogold labeling was still detected in the chloroplasts of the subepidermic cell layer and the amyloplasts of the internal starch sheath layer (Figure 4E), whereas the vascular bundles were only weakly stained (Figures 4E and 4F).

To confirm that the amount of GS protein was specifically impaired in the vascular tissue of transgenic plants, GS also was localized using transmission electron microscopy. Figures 5D to 5F show that labeling in the cytoplasm of phloem cells was just above the background level (Figure 5G) in SOD-AS–transformed plants, whereas in the untransformed control plants, gold particles were abundant within the companion cells (Figures 5B and 5C). Other organelles, such as mitochondria, remained unstained. In contrast, the amount of GS2 within the chloroplast stroma of the subepidermic cell layer was not significantly different in stems of either transformed or untransformed control plants. Figure 5A shows the intense labeling in the chloroplast stroma in SOD-AS–transformed plants. Similar results were obtained in untransformed control plants (data not shown).

We also studied GS localization in root tissues of untransformed control plants and SOD-AS–transformed plants by using transmission electron microscopy–immunogold labeling. The pattern of GS distribution in epidermal and cortical root cells was similar in both control and SOD-AS plants. We observed a very high concentration of GS1 in epidermal cells and a slightly lower concentration in external cortical cells. The quantity of GS1, as determined by the density of gold particles, was unchanged in the root epidermis and cortex of SOD-AS plants (Figure 6A). In accordance with the amount of GS2 (45 kD) detected by protein gel blot analyses, we also observed a high degree of labeling in the plastids (Figure 6A). The quantity of GS in the plastids was similar to that of control plants (Figure 6B). In the root central cylinder of SOD-AS plants, we found an extremely low level of GS1. We focused our investigation particularly on the phloem companion cells and found that this cell type was completely unlabeled (Figures 6C and 6D). In contrast, within the phloem companion cells of control plants, we observed uncontestable cytosolic labeling (Figures 6E and 6F), although the labeling intensity did not reach the level observed in stem or leaf tissues (Figure 5).

Additional experiments were performed with two transgenic lines in which the same antisense *Gln1-5*–specific mRNA fragment was expressed under the control of the cauliflower mosaic virus (CaMV) 35S promoter. In terms of both gene expression and protein distribution, similar results were obtained in comparison with the SOD-AS antisense plants (data not shown).

Physiology of the SOD-AS Transgenic Plants

To determine the effect of decreased levels of GS activity in the phloem on ammonia assimilation and amino acid biosynthesis and transport, transgenic and control plants were first grown for 8 weeks on a nitrate-containing solution (N12

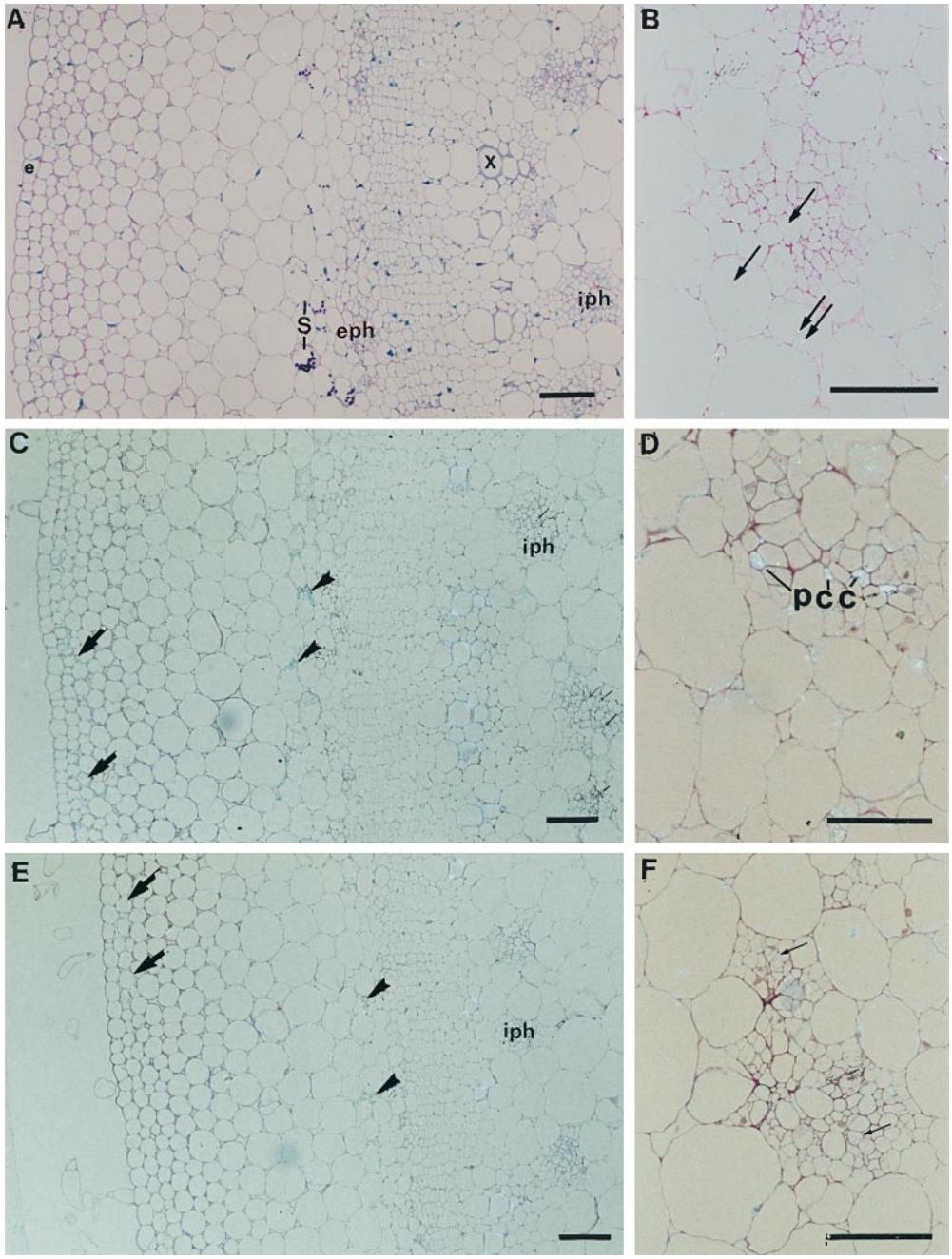

Figure 4. Histochemical and Immunolocalization of GS in Stems of SOD-AS–Transformed and Untransformed Tobacco Plants.

In experiments using immunogold labeling followed by silver enhancement, similar results were obtained for both SOD-AS7– and SOD-AS9–transformed plants.

(A) Histological presentation of a stem section, using PAS-NBB staining, showing different tissues such as the epidermis, the starch sheath cells, the external phloem, the xylem, and the internal phloem.

(B) Control section treated with normal rabbit serum instead of anti-GS serum the specificity of labeling. Only a weak background signal was observed (arrows).

(C) Immunolocalization of GS in a section of untransformed tobacco stem. Labeling was observed in the subepidermal cell layer (large arrows), cells of the starch sheath layer (arrowheads), and some internal phloem cells (thin arrows). The white autofluorescence corresponds to the lignified xylem vessels.

(D) Magnification of the internal phloem zone presented in **(C)** showing intense labeling in the phloem companion cells.

(E) Immunolocalization of GS in stems sections of SOD-AS–transformed plants. Labeling also was observed in the subepidermal cell layer (large arrows) and cells of the starch sheath layer (arrowheads). No apparent labeling was visible in the internal phloem.

(F) Magnification of the internal phloem zone presented in **(E)** showing very weak labeling in phloem companion cells (arrows).

e, epidermis; eph, external phloem; iph, internal phloem; pcc, phloem companion cells; S, sheath cells; x, xylem. Bars = 50 μm.

solution) and then forced to assimilate large amounts of ammonium after a transfer to a complete nutrient solution containing 8 mM NH_4^+ as the sole nitrogen source for an additional 2 weeks. Because many plants differ with respect to ammonium tolerance (Salsac et al., 1987), untransformed plants were initially tested for their ability to grow under different NH_4^+ concentrations. A concentration of 8 mM was selected for this study because after 2 weeks, it did not significantly modify plant growth and development. Moreover, no effect on growth was apparent in plants with reduced GS activity in the phloem (data not shown).

Compared with untransformed controls, no significant differences in the total amino acid concentration were observed in leaves, stems, roots, xylem sap, or phloem sap of transgenic plants (Tables 2 and 3). However, proline concentration and proportion were significantly decreased (between 35 and 75%) in roots, stems, and leaves and in the phloem sap and xylem sap of transgenic plants when compared with controls (Tables 2 and 3). Similar results were obtained with respect to the proline content in transgenic plants expressing the *GS* antisense mRNA under the control of the CaMV 35S promoter (data not shown). The relative concentrations of asparagine and glutamate were not significantly different in transgenic plants, except in the xylem sap, in which asparagine concentration doubled from that seen in the controls. A 25% decrease in glutamine in roots and a 25% increase in serine and aspartate in most organs and in the phloem sap were detected in GS antisense plants.

A $^{15}NH_4^+$-labeling experiment was then conducted, and the dynamics of primary ammonia assimilation were examined in a pulse (^{15}N)–chase (^{14}N) experiment over a 48-hr period to determine whether decreased GS activity in the phloem had also modified the dynamics of proline accumulation. Both untransformed control plants and transgenic plants were fed for 48 hr with a nutrient solution containing 8 mM $^{15}NH_4^+$ (50% ^{15}N/total N). This pulse period was followed by a 48-hr chase period on 8 mM $^{14}NH_4^+$. This pulse–chase experiment allowed the tracing of exogenous and endogenous nitrogen, and it also showed the dynamics of nitrogen transfer between various amino acids pools, such as those of proline, glutamine, and glutamate. In untransformed tobacco plants, a significant increase in proline content accompanied by a concomitant decrease in the glutamine pool was clearly visible during the 48-hr chase period (Figure 7). In contrast, the pool of glutamate showed a small (but significant) increase.

This result suggests that glutamine was used as a precursor for the synthesis of proline via glutamate. The latter assumption is strengthened by the simultaneous increase in ^{15}N-proline and decrease in ^{15}N-glutamine, which demonstrates that most of the proline synthesized during the chase period is derived from a preexisting pool of glutamine. Furthermore, the net decrease in the glutamine pool indicates that the balance between the reactions leading to the synthesis of glutamine and the synthesis of proline was in favor of the latter. This observation confirms the hypothesis that proline may constitute a strong sink for amino-nitrogen in plants when a pulse of ammonia is provided to the plant (Ahmad and Hellebust, 1988; Singh, 1993). Compared with untransformed plants, glutamate, which apparently represents an intermediary pool between glutamine and proline, was increased in transformed plants. However, the low but significant decrease in ^{15}N-glutamate indicates that its rate of use was almost similar to its rate of synthesis. In contrast, both the absence of proline accumulation and nitrogen-15 labeling of proline in transgenic plants confirmed that its synthesis was strongly reduced. Compared with untransformed control plants, the greater decrease in both glutamine content and nitrogen-15 labeling of glutamine indicates that during the chase period, the preexisting pool of glutamine was used more extensively in transgenic plants. In contrast, the use of glutamate was similar to that of the control plants (Figure 7).

Phenotypic Effect of Salinity Stress on Transgenic Plants

Proline is thought to play an important role as an osmoregulatory solute in plants subjected to drought and salt stress (Delauney and Verma, 1993) and in stabilizing cellular structures as well as scavenging free radicals (Hare and Cress, 1997). Because antisense plants lacking GS activity in the phloem had decreased proline content, we decided to look at their phenotype after salt stress. Plants from each T_1 transgenic line (SOD-AS7 and SOD-AS9) and untransformed control plants were first grown for 8 weeks on N12 solution. Ten individuals of the same size and at the same stage of development in the three sets of plants were grown for an additional 2 weeks on the same growth medium supplemented with 25 mM NaCl. For the two transgenic lines, at least half of the plants displayed a pronounced stress phenotype, consisting of wilting and bleaching in the older leaves (Figures 8A and 8B), whereas the rest of the plants displayed variable degrees of stress phenotype. After 2 weeks of salt treatment, the control plants were uniform, showing no symptoms of stress (Figure 8C). Proline, glutamate, and glutamine concentrations were measured in the youngest leaves that did not show a visible stress phenotype. The concentration of proline in leaves of transgenic plants was half that of the controls. The respective levels of glutamate and glutamine were similar in both transgenic and untransformed control plants (Table 4).

DISCUSSION

The antisense strategy (reviewed in Bourque, 1995) has been successfully employed to inhibit the expression of

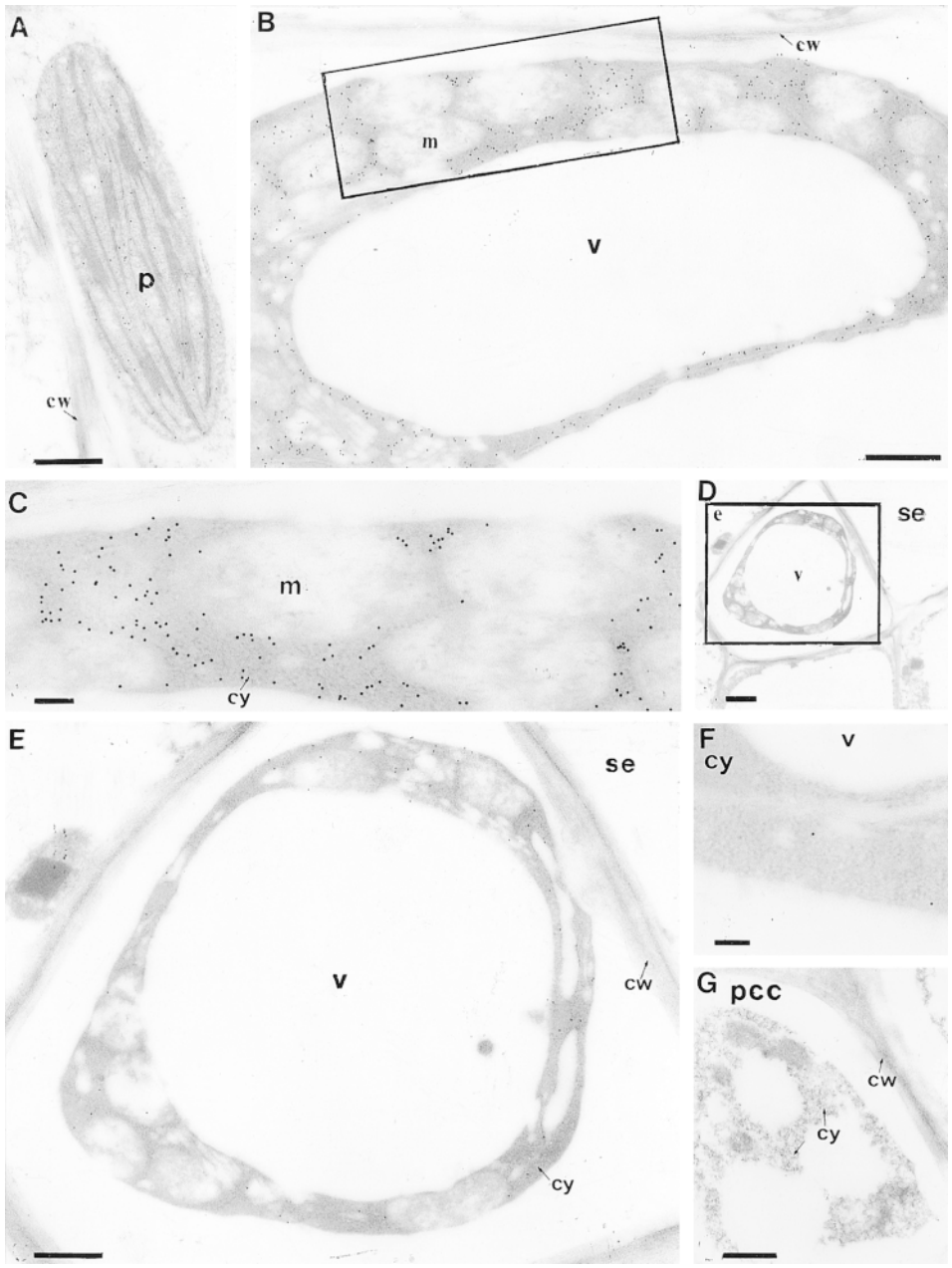

Figure 5. Immunolocalization of GS by Electron Microscopy in Stems of SOD-AS Transgenic Tobacco Plants and Untransformed Control Plants.

Similar results were obtained with both SOD-AS7– and SOD-AS9–transformed plants.
(A) Labeling in chloroplasts of the subepidermal cells layer of SOD-AS–transformed plants.
(B) and **(C)** Localization of GS in the cytosol of phloem companion cells of untransformed control plants. The boxed area indicates the zone magnified in **(C)**. Note that the cytoplasm was strongly labeled, whereas mitochondria and cell walls remain unlabeled. **(C)** provides a view of the cytoplasm of labeled companion cells of untransformed control plants.
(D) and **(E)** Localization of GS in the cytoplasm of phloem companion cells of SOD-AS–transformed plants. The boxed area indicates the zone magnified in **(E)**. A phloem companion cell of a SOD-AS–transformed plant showing weak labeling in the cytoplasm is shown in **(E)**.
(F) Close-up view of the cytoplasm of a companion cell of a SOD-AS–transformed plant exhibiting very weak labeling. For comparison with untransformed control plants, see panel **(C)**.
(G) Control section incubated with preimmune serum. Note that only a few gold particles are visible.
cw, cell wal; cy, cytolsol; m, mitochondria; p, chloroplasts; pcc, phloem companion cells; se, sieve elements; v, vacuole. Bars in **(A)**, **(B)**, and **(E)** = 0.5 μm; bars in **(C)** and **(F)** = 0.1 μm; bars in **(D)** and **(G)** = 1 μm.

genes involved in a variety of metabolic pathways, such as nitrate reduction (Vaucheret et al., 1992), ammonium assimilation (Temple and Sengupta-Gopalan, 1997), and carbon assimilation (Rodermel et al., 1988; Quick et al., 1991) as well as floral pigmentation (Mol et al., 1989). To evaluate the physiological impact of decreased GS activity in the phloem of plants, an antisense *GS* gene was specifically expressed in the vascular tissue of tobacco. This antisense approach was effective in silencing both *GS1* gene expression and GS1 activity in the phloem of transgenic tobacco plants. Similar results were obtained when the CaMV 35S promoter, which is able to confer a specific expression of *Gln1-5* antisense mRNA in the phloem tissues of mature tobacco plants (Benfey et al., 1990), was used rather than the Cu/Zn *SOD* promoter (data not shown). The mechanism by which antisense inhibition operates is still not fully understood, because it can affect a variety of regulatory processes, including mRNA synthesis, transport, or translation (Bourque, 1995). In this study, we showed that in the two transgenic lines exhibiting reduced midrib GS activity, both the native transcripts and the antisense mRNAs were lacking. This finding strongly suggests that a degradation of a native mRNA–antisense RNA duplex had occurred.

In chlorophyllous tissues, neither the steady state *GS2* mRNA content nor GS2 content or activity was affected by the antisense inhibition of *GS1* expression. An RNase protection assay clearly showed that the steady state amount of *Gln1-5* transcripts encoding GS1 specifically expressed in the phloem was decreased in tobacco plants expressing the antisense *Gln1-5* RNA. This experiment demonstrates that by using a specific DNA sequence fused to a promoter directing tissue-specific expression, it is possible to target the synthesis of antisense transcripts to inhibit specifically the expression of a single member in a multigene family. Although this strategy rarely has been successful in higher plants (Bourque, 1995), we demonstrate in this study that it can be a useful tool to explore the physiological role of a single component of an isoenzymatic system. Attempts to downregulate GS in the phloem were made by Temple et al. (1994) by introducing a construct consisting of an Arabidopsis acid chitinase promoter driving the expression of a *GS1* cDNA from alfalfa placed in the antisense orientation. Relatively few transformants were selected from this experiment. These transformants exhibited severe symptoms of nitrogen deficiency, which most probably were due to a general decrease of GS activity within the plant. Moreover, these authors did not clearly demonstrate that GS expression was impaired specifically in the vascular tissue, complicating the interpretation of results from the transgenic plants (Temple et al., 1994; Temple and Sengupta-Gopalan, 1997).

In this study, the main consequences of the impairment of GS activity in the phloem of tobacco plants was the significant decrease in proline in roots, stems, and leaves when ammonium was fed to the transgenic plants after culture on standard N12 nutrient solution to boost the flux of reduced nitrogen through the GS/glutamate synthase pathway. In contrast, the relative steady state levels of the major amines and amides such as glutamate, glutamine, aspartate, and asparagine were similar or only slightly modified.

An increase, related to control, in the asparagine concentration in the xylem exudates of transgenic plants suggests that more asparagine was exported from the roots to the shoots. A significant increase in aspartate and serine concentrations (from 20 to 35%) was also observed in most plant organs and in the phloem sap of transgenic plants. This may result from a transient increase in glutamate, which may then be rapidly metabolized by the enzyme aspartate aminotransferase and by the photorespiratory nitrogen cycle in response to an excess of ammonia (Canvin and Salon, 1997). Interestingly, this increase was more pronounced in chlorophyllous tissues and in the phloem sap, which suggests that this could provide means of maintaining a constant rate of glutamate synthesis and export in photosynthetic tissues.

Therefore, it can be concluded that the major consequence of decreased GS in the phloem, in terms of amino acid content and transport, is a decrease in the amount of proline present in different organs or transported within the plant. This observation confirms the hypothesis that synthesis of proline (Raab and Terry, 1995), rather than synthesis of arginine, glutamine, or asparagine, may be a means of assimilating excess ammonium, acting as an additional mode of nitrogen storage (Ahmad and Hellebust, 1988; Singh, 1993). In particular, a marked (up to threefold) decrease was observed in the proline content of the phloem sap and the xylem sap. This observation suggests that a decrease in proline synthesis may have occurred in both shoots and roots, which are the major sites of proline synthesis (Hua et al., 1997). Moreover, the large decrease in proline in the xylem sap confirms the hypothesis of Hua et al. (1997), who suggested that proline synthesized in roots is exported to other parts of the plant.

In higher plants, proline synthesis is catalyzed by the enzymes Δ^1-pyrroline-5-carboxylate synthetase (Hu et al., 1992) and Δ^1-pyrroline-5-carboxylate reductase, which use glutamate as a substrate (Delauney and Verma, 1993). Proline synthesis occurs in various cellular compartments in roots and leaves (Szoke et al., 1992). Transgenic tobacco plants overexpressing Δ^1-pyrroline-5-carboxylate synthetase (Kishor et al., 1995) exhibited increased proline synthesis. However, it was not determined in this study whether the availability of either glutamate or glutamine was an important limiting factor for proline production because the type of analysis that was performed did not differentiate between the two amino acids.

To determine which step in glutamate recycling was limiting for proline production, a $^{15}NH_4^+/^{14}NH_4^+$ pulse–chase experiment was performed with both untransformed control plants and SOD-AS plants. This experiment confirmed that proline synthesis was strongly reduced in transgenic plants but showed that glutamine rather than glutamate is the major amino acid used for proline synthesis via a constant pool

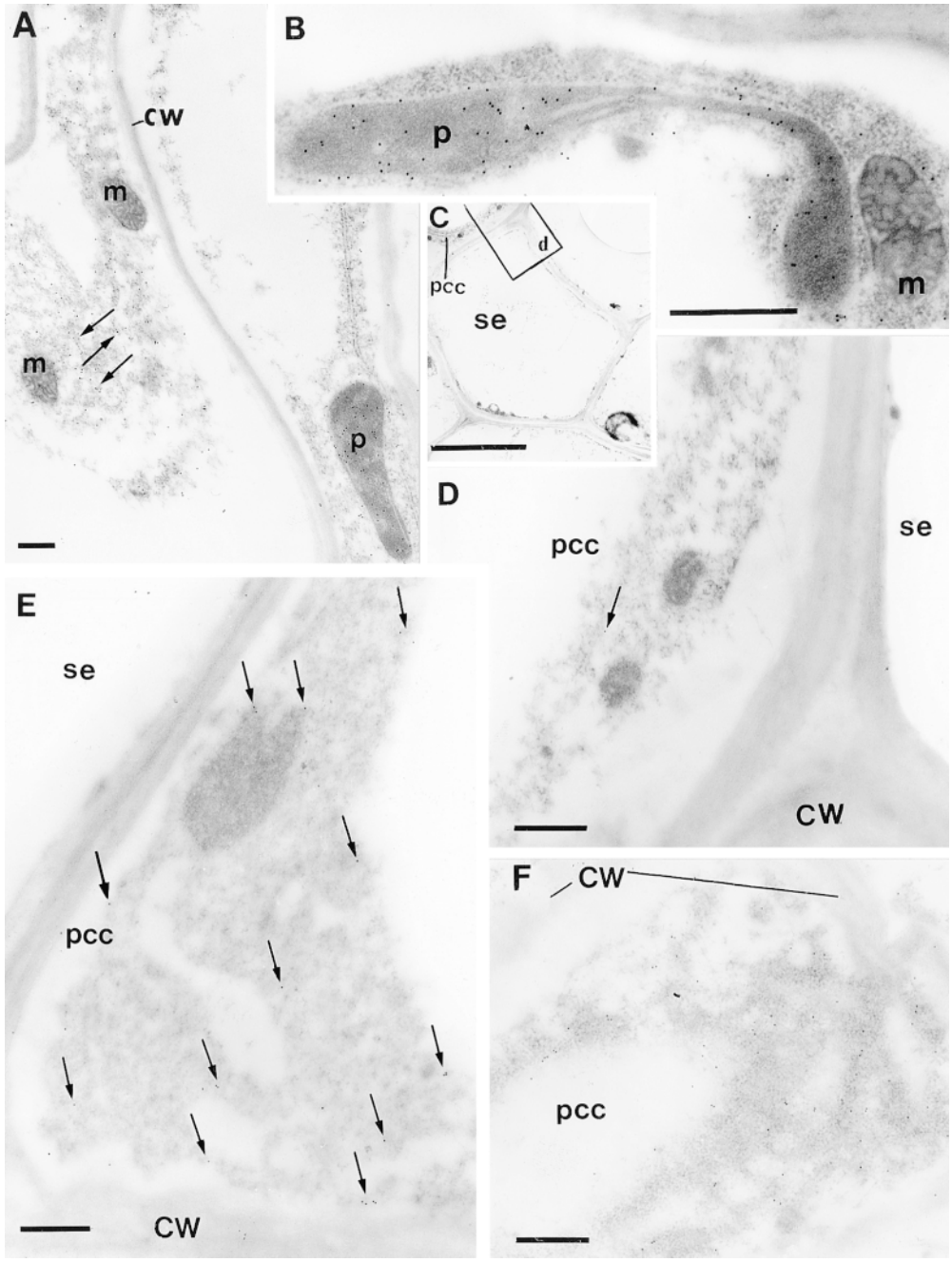

Figure 6. Immunolocalization of GS by Electron Microscopy in Roots of SOD-AS–Transformed and Untransformed Control Tobacco Plants.

Similar results were obtained with both SOD-AS7– and SOD-AS9–transformed plants.
(A) Heavy labeling in the cytoplasm of an SOD-AS epidermal cell (arrows indicate some of the numerous gold particles). Note also heavy labeling observed in the plastids of an external cortical cell.
(B) Heavy labeling in the plastid of a root external cortical cell of an untransformed control plant.
(C) and **(D)** Overall view **(C)** and detail **(D)** of a phloem companion cell in a SOD-AS–transformed plant. The arrow shows the only gold particle observed.
(E) and **(F)** Localization of GS in the cytosol of phloem companion cells of untransformed control plants. Arrows indicate the gold particles observed.
CW, cell wall; m, mitochondria; p, plastids; pcc, phloem companion cells; se, sieve elements. Bars in **(A)** and **(D)** to **(F)** = 0.5 μm; bar in **(B)** = 0.1 μm; bar in **(C)** = 5 μm.

Table 2. Concentration and Proportion of Amino Acids in Leaves, Stems, and Roots of Control and SOD-AS Antisense Plants

Amino Acids	Amino Acid Concentration (nmol/mg Dry Weight) and Proportions (%)[a]								
	Leaves			Stems			Roots		
	UT	SOD-AS7	SOD-AS9	UT	SOD-AS7	SOD-AS9	UT	SOD-AS7	SOD-AS9
Asp	1.0 (0.9)	1.0 (0.6)	0.7 (0.4)	6.7 (3)[b]	14.0 (7.7)[b]	15.6 (8.2)[b]	2.6 (4.2)	2.3 (4.6)	2.7 (5.1)
Asn	3.8 (3.4)	4.5 (2.8)	4.6 (2.8)	24.4 (11)	19.0 (10.4)	22.2 (11.7)	3.7 (6.1)	1.5 (3)	1.5 (2.8)
Glu	1.2 (1.1)	1.0 (0.6)	1.1 (0.7)	10.9 (4.9)	16.2 (8.9)	13.4 (7)	5.3 (8.6)	4.2 (8.5)	3.6 (6.8)
Gln	8.8 (8)	16.5 (10.5)	20.7 (12.9)	80.5 (36.4)	67.6 (37)	60.2 (31.8)	16.0 (25.9)	10.3 (20.9)	9.1 (17.3)
Pro	36.5 (33.4)[b]	26.0 (16.4)[b]	24.0 (15)[b]	62.5 (28.2)[b]	35.1 (19.3)[b]	32.3 (17)[b]	4.1 (6.7)[b]	2.1 (4.2)[b]	2.3 (4.3)[b]
Ser	23.8 (21.8)[b]	43.2 (27.5)[b]	47.6 (29.7)[b]	13.4 (6.1)	15.1 (8.3)	17.7 (9.3)	4.6 (7.4)	4.5 (9.1)	4.9 (54)
Others	34.4 (31.9)	65.6 (41.7)	61.5 (38.4)	22.5 (10.4)	14.0 (7.7)	27.6 (14.6)	24.6 (41.1)	24.4 (49)	28.4 (54)
Total	109±25 (100)	157±35 (100)	160±28 (100)	221±31 (100)	181±32 (100)	189±14 (100)	61.3±6 (100)	49.3±5 (100)	52.5±7 (100)

[a] Amino acids were separated and quantified in tobacco plants grown for 8 weeks on a complete N12 solution and for an additional 2 weeks on 8 mM NH_4^+ as sole nitrogen source. Values are the mean of six untransformed control plants (UT) and the two SOD-AS7 and SOD-AS9 transgenic lines for which three individual plants were analyzed (SOD-AS). Relative amino acid proportions are given in parentheses. Standard deviation for the individual amino acids was of the same order of magnitude when compared with the total amino acids.
[b] Significant changes in the amino acid proportions.

of glutamate. The lack of GS activity in the phloem of SOD-AS transgenic plants is likely to provoke a shortage in glutamine, which preferentially may be used for export and/or as an amino group donor rather than for proline synthesis. In this experiment, the increase in the glutamate pool over a 48-hr period may be explained by a lessened amount of recycling through the glutamate synthase reaction in response to the shortage of glutamine. The increase in glutamate was not observed when amino acid steady state levels were measured after ammonia was provided to the plants, indicating that it was transient. These observations agree with the work of Rhodes et al. (1986), who showed that even when large quantities of proline were synthesized, glutamine, which constitutes a metabolically inactive storage pool, was the only amino acid to exhibit a significant decline in response to water stress.

These observations led us to propose that GS in the phloem plays a major role in regulating proline synthesis. This hypothesis is consistent with the recent work of Larher et al. (1998), who showed that application of a GS inhibitor to leaf discs prevented conversion of amino acids to proline. Furthermore, the phenotype observed in transgenic plants fed with 25 mM NaCl indicates that they were less tolerant of salt stress. In the youngest leaves of transgenic plants that are the major site of amino acid accumulation (including proline; Dungey and Davis, 1982; Fukutoku and Yamada,

Table 3. Concentration and Proportion of Amino Acids in Phloem Sap and Xylem Sap of Control and SOD-AS Antisense Plants

Amino Acids	Amino Acid Concentration (nmol/mL) and Proportions (%)[a]					
	Phloem Exudate			Xylem Exudate		
	UT	SOD-AS7	SOD-AS9	UT	SOD-AS7	SOD-AS9
Asp	54.9 (5.1)[b]	94.8 (8.7)[b]	103.0 (9.1)[b]	35.8 (1.8)	31.2 (2.0)	32.4 (1.9)
Asn	47.9 (4.4)	42.1 (3.9)	46.1 (4.1)	195.0 (9.8)[b]	230.0 (15.1)[b]	248.0 (15.3)[b]
Glu	75.6 (7)	93.2 (8.6)	95.0 (8.4)	71.1 (3.6)	59.0 (3.9)	51.0 (3.1)
Gln	96.5 (8.9)	121.0 (11.1)	113.0 (9.9)	669.0 (33.6)	605.0 (39.8)	645.0 (39.6)
Pro	393.0 (36.5)[b]	251.0 (23.1)[b]	269.0 (23.7)[b]	288.0 (14.5)[b]	79.1 (5.2)[b]	69.3 (4.3)[b]
Ser	233.0 (21.6)[b]	340.0 (31.3)[b]	359.0 (31.7)[b]	108.0 (5.4)	78.0 (5.1)	72.0 (4.4)
Others	177.0 (16.4)	143.0 (13.2)	149.0 (13.1)	624.0 (31.3)	438.0 (28.8)	509.0 (31.3)
Total	1078±112 (100)	1085±48 (100)	1134±108 (100)	1990±182 (100)	1520±106 (100)	1627±139 (100)

[a] Amino acids were separated and quantified in tobacco plants grown for 8 weeks on a complete N12 solution and for an additional 2 weeks on 8 mM NH_4^+ as sole nitrogen source. Values are the mean of six untransformed control plants (UT) and the two SOD-AS7 and SOD-AS9 transgenic lines for which three individual plants were analyzed (SOD-AS). Relative amino acid proportions are given in parentheses. Standard deviation for the individual amino acids was of the same order of magnitude compared with total amino acids.
[b] Significant changes in the amino acid proportions.

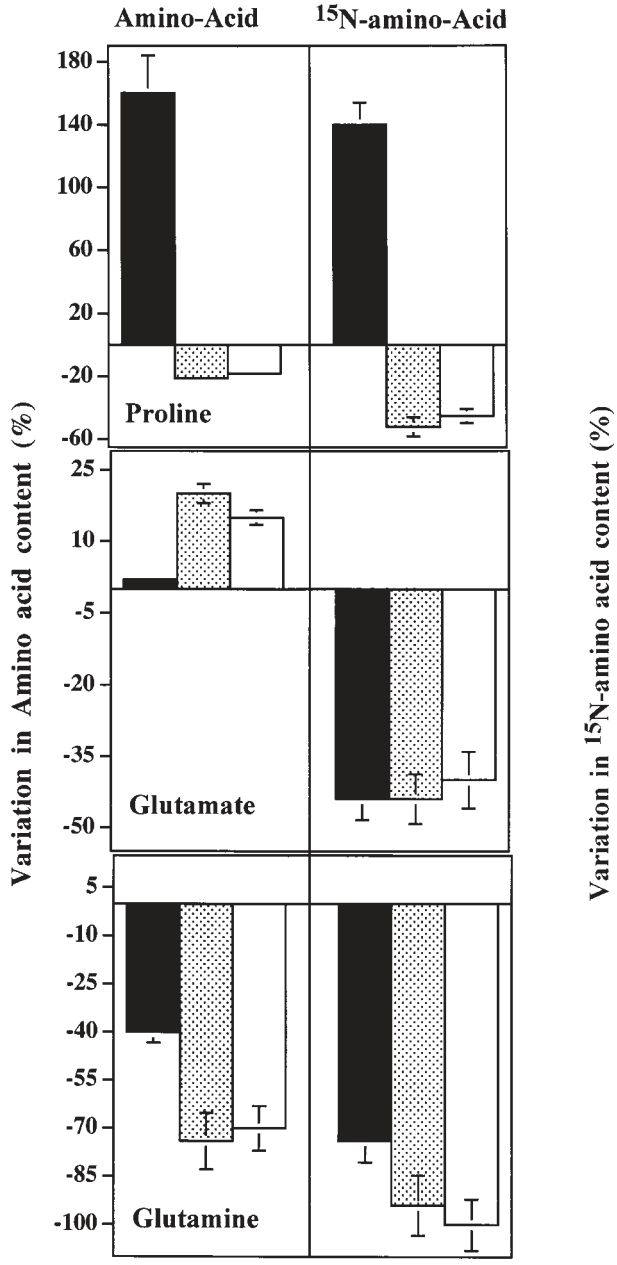

Figure 7. Evolution of Proline, Glutamate, and Glutamine Pool Sizes and Nitrogen-15 Abundance in Tobacco Leaves over a 48-Hr Period.

Plants were labeled for 48 hr with $^{15}NH_4Cl$ (pulse period) and grown for an additional 48 hr on $^{14}NH_4Cl$ (chase period). The evolution of the proline, glutamate, and glutamine pools and their respective nitrogen-15 content was measured between the pulse and chase periods. Values expressed as a percentage of the maximum are the mean (±SD) of four untransformed control plants (filled) and two SOD-AS7 (stippled) and SOD-AS9 (open) transgenic lines for which two individual plants were analyzed.

1984), amino acid analysis showed that proline was less abundant.

Our study represents a significant contribution toward a better understanding of the mechanisms controlling proline production in higher plants and demonstrates that the regulation of this metabolic pathway may be controlled by the availability of glutamine in specialized cellular structures, such as the phloem. To determine the regulation and signaling of nitrogen remobilization and recycling under water stress conditions (Bauer et al., 1997), further molecular and physiological studies will be conducted using either transgenic plants or mutants affected in the pathway of ammonia assimilation.

METHODS

Plant Material

Tobacco (*Nicotiana tabacum* L. var Xanthi) plants were grown in a controlled environment growth chamber (16 hr of light, with 150 to 200 μmol of photons m^{-2} sec^{-1}, at 26°C, and 8 hr of darkness at 18°C). Seeds of control plants and transgenic lines were sown on MS (Murashige and Skoog, 1962) medium or MS medium containing kanamycin (200 μg/mL), respectively, and grown in vitro for 15 days. Plantlets were then transferred to sand and grown for 8 weeks in a growth chamber in N12 solution (10 mM NO_3^- and 2 mM NH_4^+; Coïc and Lesaint, 1971). After this period, plants were grown for an additional 2 weeks with an 8 mM NH_4^+ complete solution containing 1.25 mM K^+, 0.25 mM Ca^+, 0.25 mM Mg^{2+}, 1.25 mM $H_2PO_4^-$, 21.5 μM iron (Sequestrene; Ciba-Geigy, Basel, Switzerland), 23 μM boron, 9 μM manganese, 0.3 μM molybdenum, 0.95 μM copper, and 3.5 μM zinc. Ammonium was supplied as 1.5 mM $(NH_4)_2SO_4$ plus 1 mM $NH_4H_2PO_4$ plus 4 mM NH_4Cl. Plants were automatically watered for 1 min (flow rate for each plant of 50 mL/min) every 2 hr during the day and every 4 hr during the night.

Construction of the Chimeric *SOD-AS* Gene

The SstI-BamHI fragment of 274 bp from the coding region of the *Gln1-5* tobacco cDNA (EMBL accession number X95932; Dubois et al., 1996) was cloned into a BamHI-SstI–cut (devoid of β-glucuronidase) pBI121 plasmid (Jefferson et al., 1987) to obtain pBI-35S-AS. The *SOD* promoter from *Nicotiana plumbaginifolia* was excised from pCZ12*SOD* (Hérouart et al., 1993) using a HindIII-HincII digest and subcloned into HindIII-EcoRV–cut pBluescript SK^+ (Stratagene, La Jolla, CA). The resulting pBS-SOD plasmid was then digested by HindIII and BamHI, and the fragment containing the promoter was cloned into HindIII-BamHI–cut pBI-35S-AS (devoid of the 35S promoter) to give the pBI-*SOD-AS* vector.

Plant Transformation

The pBIN19-derived vector containing the *SOD-AS* construct in *Escherichia coli* DH5α (Maniatis et al., 1982) was transferred to *Agrobacterium tumefaciens* (strain LBA4404) (Bevan, 1984) via triparental mating using pRK2013 as a helper (Ditta et al., 1980). The transfor-

Figure 8. Phenotype of Control and SOD-AS–Transformed Plants Subjected to Salinity Stress.

(A) Transgenic line SOD-AS7.
(B) Transgenic line SOD-AS9.
(C) Untransformed control plants.
Plants were grown on an N12 solution (see Methods) for 8 weeks and then transferred to an N12 solution supplemented with 25 mM NaCl for another 2 weeks.

mants selected on kanamycin were used to inoculate leaf discs of *N. tabacum* (Horsch et al., 1985), and transformed callus and shoots were selected on MS (Murashige and Skoog, 1962) medium containing kanamycin (200 μg/mL). Transformed shoots were rooted on MS medium containing kanamycin, transferred to the greenhouse, and grown for 8 weeks with the Coïc and Lesaint solution (Coïc and Lesaint, 1971). At this stage, midribs from independently transformed plants and untransformed control plants were harvested and stored in a −80°C freezer until used for RNA extraction. The plants were self-fertilized and allowed to set seed. The resulting T_1 progeny were used to study the physiology of the antisense plants.

RNA Gel Blot Analysis and S1 Protection Assay

Total RNA was isolated from 0.5 to 1 g of frozen *N. tabacum* plant material using a hot phenol extraction procedure and a selective precipitation with 4 M LiCl to remove traces of DNA and small RNA species (Verwoerd et al., 1989). For gel blot experiments, total RNA samples were prepared as described by Becker et al. (1993). For staining, 1 μL of a solution containing 10 mg mL^{-1} of ethidium bromide was added to each denatured RNA sample. Electrophoretic separation was performed on 1.5% agarose gels containing 5% (v/v) of a solution of 37% formaldehyde in Mops buffer (0.02 M Mops, pH 7.0, 5 mM sodium acetate, and 1 mM EDTA). Gels were blotted onto GeneScreen membranes (New England Nuclear Research Products, Boston, MA) and hybridized with random-primed ^{32}P-labeled probes (Prime-It RmT; Stratagene). Hybridizations were performed at 65°C in 50 mM Tris-HCl, pH 7.5, 0.2% serum albumin, 0.2% PVP (M_r of 40,000), 0.2% Ficoll (molecular weight of 400,000), 0.1% sodium pyrophosphate, 1% SDS, 6% NaCl, and 100 μg/mL denatured calf thymus DNA. Filters were washed twice with 2 × SET (0.06 M Tris-HCl, pH 7.6, 0.3 M NaCl, and 4 mM EDTA) for 5 min at room temperature with constant agitation and once at 65°C for 30 min. Additional washings were done successively with 1 × SET, 0.5 × SET, and 0.25 × SET at 65°C for 20 min; the filters were then dried and exposed to x-ray film (Biomax MS; Kodak). Quantitative analyses were done using an Advanced Quantifier (Bio Image, Ann Arbor, MI).

S1 protection assays were conducted according to Coruzzi et al. (1984) with a ^{32}P-labeled single-stranded RNA probe synthesized in vitro using SP6 polymerase (SP6/T7 transcription kit; Boehringer Mannheim) and ^{32}P-UTP (Du Pont–New England Nuclear, Boston, MA), as described by Dubois et al. (1996).

Protein Extraction, Fractionation, Enzymatic, Assay, and Protein Gel Blot Analyses

All operations were performed at 4°C. Leaves, stems, or roots of each plant were harvested and stored at −80°C until use. Samples

Table 4. Concentration and Proportion of Amino Acids in Young Developing Leaves of Control and SOD-AS Antisense Plants Treated with Salinity Stress

Amino Acids	Amino Acid Concentration (nmol/mg Dry Weight) and Proportions (%)[a]		
	UT	SOD-AS7	SOD-AS9
Glu	19.0 (12.4)	21.5 (12.9)	24.5 (17.3)
Gln	15.8 (10.3)	19.2 (11.5)	22.4 (15.8)
Pro	18.0 (11.8)[b]	10.3 (6.2)[b]	8.5 (6.0)[b]
Others	100.2 (65.5)	116.0 (69.5)	86.0 (60.8)
Total	153 ± 18 (100)	167 ± 17 (100)	141 ± 39

[a] Amino acids were separated and quantified in tobacco plants grown for 8 weeks on a complete N12 solution and transferred for an additional 2 weeks into the same solution supplemented with 25 mM NaCl. Values are the mean of six untransformed control plants (UT) and the two SOD-AS7 and SOD-AS9 transgenic lines for which three individual plants were analyzed (SOD-AS). Relative amino acid proportions are given in parentheses. Standard deviation for the individual amino acids was of the same order of magnitude compared with total amino acids.
[b] Significant changes in the amino acid proportions.

were ground in liquid nitrogen (5 mL/g fresh tissue), and the powder was transferred to an ice-cold mortar containing extraction buffer (25 mM Tris-HCl, pH 7.6, 1 mM $MgCl_2$, 1 mM EDTA, 14 mM β-mercaptoethanol, and 1% [w/v] of Polyclar AT (Sigma) and ground until homogenization. The slurry was filtered through Miracloth (Calbiochem, San Diego, CA) and centrifuged at 30,000*g* for 30 min. The supernatant was assayed for glutamine synthetase (GS) activity, as described by Guiz et al. (1979). Protein concentration of tissue extracts was determined by the method of Bradford (1976). Proteins were fractionated by SDS-PAGE (10% polyacrylamide) according to Laemmli (1970). The denaturated proteins were then electrophoretically transferred onto a nitrocellulose membrane (Schleicher and Schuell), as described by Towbin et al. (1979). An anti-GS2 antiserum raised in rabbits against GS2 of tobacco was used to detect GS proteins (Hirel et al., 1984). The signals were quantified by densitometric scanning using the Bio Image Advanced Quantifier 1-D Match software.

For DEAE-Sephacel (Pharmacia, Uppsala) chromatography, 2 g of stems from four wild-type plants or four SOD-AS7 or SOD-AS9 plants were ground as described above. The brei was filtered through Miracloth and centrifuged at 40,000*g* for 30 min. The supernatant was loaded (flow rate of 0.5 mL min^{-1}) onto a DEAE-Sephacel column (9 cm × 1 cm) (Econo-Column; Bio-Rad, Richmond, CA) that had been equilibrated previously in the extraction buffer without Polyclar AT. After loading, the column was washed with the same buffer for 50 min at a flow rate of 0.5 mL/min. Proteins were then eluted with a linear gradient of 0 to 0.4 M NaCl at a flow rate of 0.25 mL/min using a gradient former (Econo Pump and System Controller; Bio-Rad). Forty-eight fractions of 2 mL were collected and assayed for GS activity, as described above. Protein fractions were concentrated using microconcentrators (Microcon-3; Amicon, Beverly, MA), and protein gel blot experiments were performed as described above by using 6 μg of proteins from each fraction.

Phloem and Xylem Sap Collection

Phloem and xylem exudates were collected from *N. tabacum* plants grown as described above. Phloem exudates were obtained using the technique described by King and Zeevaart (1974). The leaves were cut off and petioles were recut under water before rapid immersion in the collection buffer. For each experiment, petioles of fully expanded leaves of three untransformed and three of each SOD-AS plants were placed separately in a solution of 10 mM Hepes and 10 mM EDTA (adjusted to pH 7.5 with NaOH) in a humid chamber (relative humidity >90%) and in the dark. Exudates were collected during 6 hr from 10:00 AM to 4:00 PM. The fresh weights of the leaves were then measured and the exudates stored at −80°C. Phloem exudates (in the EDTA solution) were adjusted to pH 2.1 and centrifuged to remove debris and EDTA, which precipitates at that pH.

For xylem sap collection, stems of plants were cut 2 cm above the root system, and the cut stem was rinsed with water and blotted dry. Root pressure bleeding sap (~200 μL per plant) was collected with a micropipette, and the samples were immediately stored at −80°C. Amino acid analysis was performed as described below.

Amino Acid Analysis

Samples of the first fully expanded leaf, stem, or root of six control or six SOD-AS plants (three of each primary line) were freeze-dried, and a 100-mg dry weight sample was agitated for 1 hr in 3 mL of 96% ethanol at 4°C. After centrifugation for 10 min at 27,000*g*, the ethanol fraction was saved. The process was repeated with 60% ethanol and finally with water. The three ethanol/water fractions were combined; aliquots were dried in a speed-vac desiccator (Savant, Holbrook, NY) and stored at −80°C until analysis. Amino acids and free ammonium were determined on water-solubilized aliquots. Samples were assayed for amino acid determination by ninhydrin (Rosen, 1957). The same quantities of amino acids were separated by ion exchange chromatography (LC 5001 analyzer; Biotronik, Maintel, Germany; lithium citrate buffers; and ninhydrin postcolumn derivatization), identified using a mixture of amino acids (Benson, Reno, NV), and quantified using the Perkin-Elmer Nelson software. Values in percentages are the mean of three independent plants.

Nitrogen-15 Labeling Experiment and Gas Chromatography and Mass Spectrometry

N. tabacum plants (four control plants and four SOD-AS transgenic plants) were grown for 8 weeks on N12 solution, as described above in Plant Material, and then watered with a nitrogen-free solution (Coïc et al., 1972) for 5 days to avoid the accumulation of inorganic nitrogen (mainly stored as nitrate in the vacuole). The plants were then watered for 48 hr with a complete nutrient solution containing 8 mM NH_4^+ (see Plant Material) and enriched with 50% $^{15}NH_4Cl$. After the labeling (pulse) period, five leaf discs of 1 cm in diameter (400 to 500 mg fresh weight) were harvested (each from a different leaf stage) from control and transgenic plants and stored at −80°C for further analysis. The root system of these plants was then extensively rinsed with an 8 mM $^{14}NH_4^+$ solution to eliminate excess $^{15}NH_4^+$ and grown for an additional 48 hr on the same nutrient solution, constituting a chase period. After this chase period, five new leaf discs were harvested in control plants and transgenic plants and stored at −80°C for further analysis. Both the evolution of their amino acid content and their respective ^{15}N enrichment were examined between the pulse and the chase period by gas chromatography coupled to mass spectrometry (GC-MS).

Amino acids were extracted using a modified procedure originally described by Lejay et al. (1997). Frozen samples (ranging from 300 to 500 mg fresh weight of tissue) were ground in liquid nitrogen and extracted at 4°C in 5 mL of methanol-chloroform (12/5 [v/v]) for 60 min. The homogenate was centrifuged at 27,000*g* for 20 min. The pellet was then extracted with 5 mL of methanol-chloroform-water (12/5/3 [v/v]), and the two supernatants were pooled. The addition of 3 mL of chloroform and 4 mL of water to the pooled supernatants allowed the separation of two phases. After centrifugation at 800*g* for 5 min, the upper methanol/water fraction was collected, freeze-dried, and redissolved in 1 mL of distilled water. The resulting samples were then applied to 5.0 × 0.5 cm Dowex-50 H^+ columns (Bio-Rad) and washed with 5 mL of distilled water. Amino acids were eluted with 4 mL of 6 M NH_4OH. The amino acid fraction was lyophilized and redissolved in the suitable buffer for either quantification of total amino acids or GC-MS analysis. Amino acid quantities were determined as described earlier. For GC-MS analysis, lyophilized amino acid samples were resuspended in 0.1 N HCl, dried under N_2, and derivatized with *N*-methyl-*N*-(tert-butyldimethylsilyl)-trifluoroacetamid (Pierce, Rockford, IL), as described by Rhodes et al. (1989). The atom percentage of nitrogen-15 of each amino acid was then determined by GC-MS analysis (model MD800; Fisons, Beverly, MA).

Immunocytochemical Studies

The different *N. tabacum* organs were fixed in freshly prepared 1.5% paraformaldehyde in phosphate buffer for 4 hr at 4°C. For immunolocalization, material was dehydrated in an ethanol series (final concentration of 80% ethanol) and then embedded in London Resin white resin (Polysciences, Warrington, PA). Polymerization was conducted in gelatin capsules at 50°C.

For structural investigations, thin sections (1 μm) were stained by the Periodic Acid Schiff's–Naphtol Blue-Black (PAS-NBB) method, as described by Sangwan et al. (1992).

For immunotransmission electron microscopy studies, ultrathin sections were mounted on 400-μm mesh nickel grids and allowed to dry at 37°C. Sections were first incubated with 5% normal goat serum in T1 buffer (0.05 M Tris-HCl buffer containing 2.5% NaCl, 0.1% BSA, and 0.05% Tween 20, pH 7.4) for 1 hr at room temperature and then with anti-GS rabbit serum diluted 1:70 in T1 buffer for 6 hr at room temperature. Sections were then washed five times with T1 buffer, two times with T2 buffer (0.02 M Tris-HCl buffer containing 2% NaCl, 0.1% BSA, and 0.05% Tween 20, pH 8.0), and incubated with 10-nm colloidal gold goat anti–rabbit immunoglobulin complex (Sigma) diluted 1:50 in T2 buffer for 2 hr at room temperature. After several washes, grids were treated with 5% uranyl acetate in water and observed with an electron microscope (model CM12; Philips, Eindhoven, The Netherlands) at 80 kV.

For immunophotomicroscopy studies, thin sections of 2 μm were floated on drops of sterile water on slides coated with Biobond (British Biocell, Cardiff, UK), and the same procedure for labeling was used, except that 1 nm, instead of 10 nm, colloidal gold goat anti–rabbit immunoglobulin complex (British Biocell) was used. Labeling became visible when silver enhancement was performed as described by the supplier (British Biocell), and sections were back stained with 1% fuchsine before microscopic observations under bright field and epipolarized light on an epifluorescent photomicroscope (Eclips 800; Nikon, Tokyo, Japan). To visualize polysaccharides, cell wall and starch sections were treated with PAS-NBB (Sigma).

For both techniques, controls were conducted either by omitting the primary antibody or by substituting it with normal rabbit serum.

ACKNOWLEDGMENTS

We thank Elisa Carrayol and François Gosse for excellent technical assistance and Didier Hérouart, who kindly provided the pCZ12SOD clone. We are indebted to Desh Pal Verma and Judith Harrison for critically reviewing the manuscript. This project was partly financed by a doctoral fellowship (No. 94675) from Ministère de la Recherche et de l'Enseignement Supérieur to N.B.

Received May 3, 1999; accepted August 7, 1999.

REFERENCES

Ahmad, I., and Hellebust, J.A. (1988). The relationship between inorganic nitrogen metabolism and proline accumulation in osmoregulatory responses of two euryhaline microalgae. Plant Physiol. **88,** 348–354.

Bauer, D., Biehler, K., Fock, H., Carrayol, E., Hirel, B., Migge, A., and Becker, T.W. (1997). A role for cytosolic glutamine synthetase in the remobilization of leaf nitrogen during water stress in tomato. Physiol. Plant. **99,** 241–248.

Becker, T.W., Caboche, M., Carrayol, E., and Hirel, B. (1992). Nucleotide sequence of a tobacco cDNA encoding plastidic glutamine synthetase and light inducibility, organ specificity and diurnal rhythmicity in the expression of the corresponding genes of tobacco and tomato. Plant. Mol. Biol. **19,** 367–379.

Becker, T.W., Perrot-Rechenmann, C., Suzuki, A., and Hirel, B. (1993). Subcellular and immunocytochemical localization of the enzymes involved in ammonia assimilation in mesophyll and bundle-sheath cells of maize leaves. Planta **191,** 129–136.

Benfey, P.N., Ren, L., and Chua, N.-H. (1990). Tissue-specific expression from CaMV 35S enhancer subdomains in early stages of plant development. EMBO J. **9,** 1677–1684.

Bernhard, W.R., and Matile, P. (1994). Differential expression of glutamine synthetase genes during the senescence of *Arabidopsis thaliana* rosette leaves. Plant Sci. **98,** 7–14.

Bevan, M. (1984). Binary *Agrobacterium* vectors for plant transformation. Nucleic Acids Res. **12,** 8711–8721.

Blackwell, R.D., Murray, A.J.S., and Lea, P.J. (1987). The isolation and characterisation of photorespiratory mutants of barley and pea. In Progress in Photosynthesis Research, J. Biggins, ed (Dordrecht, The Netherlands: Martinus Nijhoff), pp. 625–628.

Botella, J.R., Verbelen, J.P., and Valpuesta, V. (1988). Immunocytolocalization of glutamine synthetase in green leaves and cotyledons of *Lycopersicum esculentum*. Plant Physiol. **87,** 255–257.

Bourque, J.E. (1995). Antisense strategies for genetic manipulations in plants. Plant Sci. **105,** 125–149.

Bradford, M.M. (1976). A rapid and sensitive method for the quantitation of microgram quantities of protein utilizing the principle of protein–dye binding. Anal. Biochem. **72,** 248–254.

Brangeon, J., Hirel, B., and Forchioni, A. (1989). Immunogold localization of glutamine synthetase in soybean leaves, roots and root nodules. Protoplasma **151,** 88–97.

Canvin, D.T., and Salon, C. (1997). Photorespiration and CO_2-concentrating mechanisms. In Plant Metabolism, D.T. Dennis, D.H. Turpin, D.D. Lefebvre, and D.B. Layzell, eds (Harlow, UK: Addison Wesley Longman Limited), pp. 314–340.

Carvalho, H., Pereira, S., Sunkel, C., and Salema, R. (1992). Detection of a cytosolic glutamine synthetase in leaves of *Nicotiana tabacum* L. by immunocytochemical methods. Plant Physiol. **100,** 1591–1594.

Coïc, Y., and Lesaint, C. (1971). Comment assurer une bonne nutrition en eau et en ions minéraux en horticulture. Hortic. Française **8,** 11–14.

Coïc, Y., Tendille, C., and Lesaint, C. (1972). La nutrition azotée du tournesol (*Heliantus anuus*): Action sur le rendement et la composition biochimique de la graine. Agrochimica **16,** 254–263.

Coruzzi, G.M., Broglie, R., Edwards, C., and Chua, N.-H. (1984). Tissue specific and light regulated expression of a pea nuclear gene encoding the small subunit of ribulose-1-5-bisphosphate carboxylase. EMBO J. **3,** 1671–1679.

Cullimore, J.V., Gebhardt, C., Saarelainen, R., Miflin, B.J., Idler, K.B., and Barker, R.F. (1984). Glutamine synthetase of *Phaseolus*

vulgaris L.: Organ-specific expression of a multigene family. J. Mol. Appl. Genet. **2,** 589–599.

Delauney, A.J., and Verma, D.P.S. (1993). Proline biosynthesis and osmoregulation in plants. Plant J. **4,** 215–223.

Ditta, G., Stanfield, S., Corbin, D., and Helinski, D.R. (1980). Broad host range DNA cloning system for gram-negative bacteria: Construction of a gene bank of *Rhizobium meliloti.* Proc. Natl. Acad. Sci. USA **77,** 7347–7351.

Dubois, F., Brugière, N., Sangwan, R.S., and Hirel, B. (1996). Localization of tobacco cytosolic glutamine synthetase enzymes and the corresponding transcripts shows organ- and cell-specific patterns of protein synthesis and gene expression. Plant. Mol. Biol. **31,** 803–817.

Dungey, N.O., and Davis, D.D. (1982). Protein turnover in the attached leaves of non-stressed and stressed barley seedlings. Planta **154,** 435–440.

Edwards, J.W., Walker, E.L., and Coruzzi, G.M. (1990). Cell specific expression in transgenic plants reveals non-overlapping roles for chloroplast and cytosolic glutamine synthetase. Proc. Natl. Acad. Sci. USA **87,** 3459–3463.

Fukutoku, Y., and Yamada, Y. (1984). Source of proline-nitrogen in water-stressed soybean (*Glycine max*). II. Fate of ^{15}N-labeled protein. Physiol. Plant. **61,** 622–628.

Gebhardt, C., Oliver, J.E., Forde, B.G., Saarelainen, R., and Miflin, B.J. (1986). Primary structure and differential expression of glutamine synthetase genes in nodules, roots and leaves of *Phaseolus vulgaris*. EMBO J. **5,** 1428–1435.

Guiz, C., Hirel, B., Shedlofsky, G., and Gadal, P. (1979). Occurrence and influence of light on the relative proportions of two glutamine synthetases in rice leaves. Plant Sci. Lett. **15,** 271–277.

Hare, P.D., and Cress, W.A. (1997). Metabolic implications of stress-induced proline accumulation in plants. Plant Growth Regul. **21,** 79–102.

Hérouart, D., Van Montagu, M., and Inzé, D. (1993). Redox-activated expression of the cytosolic copper/zinc superoxide dismutase gene in *Nicotiana*. Proc. Natl. Acad. Sci. USA **90,** 3108–3112.

Hérouart, D., Van Montagu, M., and Inzé, D. (1994). Developmental and environmental regulation of the *Nicotiana plumbaginifolia* cytosolic Cu/Zn-superoxide dismutase promoter in transgenic tobacco. Plant Physiol. **104,** 873–880.

Hirel, B., Weatherley, C., Cretin, C., Bergounioux, C., and Gadal, P. (1984). Multiple subunit composition of chloroplastic glutamine synthetase of *Nicotiana tabacum* L. Plant Physiol. **74,** 448–450.

Hirel, B., Miao, G.H., and Verma, D.P.S. (1993). Metabolic and developmental control of glutamine synthetase genes in legume and non-legume plants. In Plant Gene Expression, D.P.S. Verma, ed (Boca Raton, FL: CRC Press Inc.), pp. 443–458.

Horsch, R.B., Fry, J.E., Hoffmann, N.L., Eichholtz, D., Rogers, S.G., and Fraley, R.T. (1985). A simple and general method for transferring genes into plants. Science **227,** 1229–1231.

Hu, C.-A.A., Delauney, A., and Verma, D.P.S. (1992). A bifunctional enzyme (Δ^1-pyrroline-5-carboxylate synthetase) catalyses the first two steps in proline biosynthesis in plants. Proc. Natl. Acad. Sci. USA **89,** 9354–9358.

Hua, X.-J., van de Cotte, B., Van Montagu, M., and Verbruggen, N. (1997). Developmental regulation of pyrroline-5-carboxylate reductase gene expression in *Arabidopsis*. Plant Physiol. **114,** 1215–1224.

Jefferson, R.A., Kavanagh, T.A., and Bevan, M.W. (1987). GUS fusions: β-Glucuronidase as a sensitive and versatile gene fusion marker in higher plants. EMBO J. **6,** 3901–3907.

Kamachi, K., Yamaya, T., Mae, T., and Ojima, K. (1991). A role for glutamine synthetase in the remobilization of leaf nitrogen during natural senescence in rice leaves. Plant Physiol. **96,** 411–417.

Kamachi, K., Yamaya, T., Hayakawa, T., Mae, T., and Ojima, K. (1992). Vascular bundle–specific localization of cytosolic glutamine synthetase in rice leaves. Plant Physiol. **99,** 1481–1486.

Kawakami, N., and Watanabe, A. (1988). Senescence-specific increase in cytosolic glutamine synthetase and its mRNA in radish cotyledons. Plant Physiol. **88,** 1430–1434.

King, R.W., and Zeevaart, J.A.D. (1974). Enhancement of phloem exudation from cut petioles by chelating agents. Plant Physiol. **53,** 96–103.

Kishor, P.B., Hong, Z., Miao, G.-H., Hu, C.-A.A., and Verma, D.P.S. (1995). Overexpression of Δ^1-pyrroline-5-carboxylate synthetase increases proline production and confers osmotolerance in transgenic plants. Plant Physiol. **108,** 1387–1394.

Laemmli, U.K. (1970). Cleavage of structural proteins during the assembly of the head of bacteriophage T4. Nature **227,** 680–685.

Lam, H.-M., Coschigano, K., Schultz, C., Melo-Oliveira, R., Tjaden, G., Oliveira, I., Ngai, N., Hsieh, M.-H., and Coruzzi, G. (1995). Use of Arabidopsis mutants and genes to study amide amino acid biosynthesis. Plant Cell **7,** 887–898.

Larher, F., Aziz, A., Deleu, C., Lemesle, P., Ghaffar, A., Bouchard, F., and Plasman, M. (1998). Suppression of osmoinduced proline response of rape seed leaf discs by polyamines. Physiol. Plant. **102,** 139–147.

Lea, P.J., and Miflin, B.J. (1974). An alternative route for nitrogen assimilation in higher plants. Nature **251,** 614–616.

Lea, P.J., Blackwell, R.D., Murray, A.J.S., and Joy, K.W. (1989). The use of mutants lacking glutamine synthetase and glutamate synthase to study their role in plant nitrogen metabolism. In Recent Advances in Phytochemistry, Vol. 23, J.E. Poulton, J.T. Romeo, and E.E. Conn, eds (New York: Plenum Press), pp. 157–189.

Lejay, L., Quilleré, I., Roux, Y., Tillard, P., Cliquet, J.-B., Meyer, C., Morot-Gaudry, J.-F., and Gojon, A. (1997). Abolition of post-transcriptional regulation of nitrate reductase activity partially prevents the decrease in leaf NO_3^- reduction when photosynthesis is inhibited by CO_2 deprivation, but not in darkness. Plant Physiol. **115,** 623–630.

Li, M.-G., Villemur, R., Hussey, P.J., Silflow, C.D., Gant, J.S., and Snustad, D.P. (1993). Differential expression of six glutamine synthetase genes in *Zea mays*. Plant Mol. Biol. **23,** 401–407.

Lightfoot, D.A., Green, N.K., and Cullimore, V.J. (1988). The chloroplast-located glutamine synthetase of *Phaseolus vulgaris* L.: Nucleotide sequence, expression in different organs and uptake into isolated chloroplasts. Plant Mol. Biol. **11,** 191–202.

Maniatis, T., Fritsch, E.F., and Sambrook, J. (1982). Molecular Cloning: A Laboratory Manual. (Cold Spring Harbor, NY: Cold Spring Harbor Laboratory Press).

McNally, S.F., and Hirel, B. (1983). Glutamine synthetase isoforms in higher plants. Physiol. Veg. **21,** 761–774.

McNally, S.F., Hirel, B., Gadal, P., Mann, A.F., and Stewart, R. (1983). Glutamine synthetases of higher plants: Evidence for a specific isoform content related to their possible physiological role and their compartmentation within the leaf. Plant Physiol. **72,** 22–25.

Mol, J.N.M., Stuitje, A.R., and van der Krol, A.R. (1989). Genetic manipulation of floral pigmentation genes. Plant. Mol. Biol. **13,** 287–294.

Murashige, J., and Skoog, F. (1962). A revised medium for rapid growth and bioassay with tobacco tissue culture. Physiol. Plant. **115,** 473–497.

Oliveira, I.C., Lam, H.-M., Coschigano, K., Melo-Oliveira, R., and Coruzzi, G. (1997). Molecular-genetic dissection of ammonium assimilation in *Arabidopsis thaliana.* Plant Physiol. Biochem. **35,** 185–198.

O'Neal, D., and Joy, K.W. (1973). Localization of glutamine synthetase in chloroplasts. Nature New Biol. **246,** 61–62.

Peat, L.J., and Tobin, A. (1996). The effect of nitrogen nutrition on the cellular localization of glutamine synthetase isoforms in barley roots. Plant Physiol. **111,** 1109–1117.

Pereira, S., Carvalho, H., Sunkel, C., and Salema, R. (1992). Immunocytolocalization of glutamine synthetase in mesophyll and phloem of leaves of *Solanum tuberosum* L. Protoplasma **167,** 66–73.

Pérez-Rodríguez, J., and Valpusta, V. (1996). Expression of glutamine synthetase genes during natural senescence of tomato leaves. Physiol. Plant. **97,** 576–582.

Peterman, T.K., and Goodman, H.M. (1991). The glutamine synthetase gene family of *Arabidopsis thaliana*: Light-regulation and differential expression in leaves, roots and seeds. Mol. Gen. Genet. **230,** 145–154.

Quick, W.P., Schurr, U., Fichtner, K., Schulze, E.-D., Rodermel, S.R., Bogorad, L., and Stitt, M. (1991). The impact of decreased Rubisco on photosynthesis, growth, allocation and storage in tobacco plants which have been transformed with antisense *rbc*S. Plant J. **1,** 51–58.

Raab, T.K., and Terry, N. (1995). Carbon, nitrogen and nutrient interactions in *Beta vulgaris* L. as influenced by nitrogen source, NO_3^- and NH_4^+. Plant Physiol. **107,** 575–584.

Rhodes, D., Handa, S., and Bressan, R.A. (1986). Metabolic changes associated with the adaptation of plant cells to water stress. Plant Physiol. **82,** 890–903.

Rhodes, D., Rich, P.J., and Brunk, D.G. (1989). Amino acid metabolism of *Lemna minor* L. Plant Physiol. **89,** 1161–1171.

Roche, D., Temple, S.J., and Sengupta-Gopalan, C. (1993). Two classes of differentially regulated glutamine synthetase genes are expressed in the soybean nodule: A nodule-specific class and a constitutively expressed class. Plant Mol. Biol. **22,** 971–983.

Rodermel, S.R., Abbot, M.S., and Bogorad, L. (1988). Nuclear-organelle interactions: Nuclear antisense gene inhibits ribulose bisphosphate carboxylase enzyme levels in transformed tobacco plants. Cell **55,** 673–681.

Rosen, H. (1957). A modified ninhydrin colorimetric analysis for amino acids. Arch. Biochem. Biophys. **67,** 10–15.

Sakurai, N., Hayakawa, T., Nakamura, T., and Yamaya, T. (1996). Changes in the cellular localization of cytosolic glutamine synthetase protein in vascular bundles of rice leaves at various stages of development. Planta **200,** 306–311.

Salsac, L., Chaillou, S., Morot-Gaudry, J.-F., Lesaint, C., and Jolivet, E. (1987). Nitrate and ammonium nutrition in plants. Plant Physiol. Biochem. **25,** 805–812.

Sangwan, R.S., Bourgeois, Y., Brown, S., Vasseur, G., and Sangwan-Norreel, B. (1992). Characterization of competent cells and early events of *Agrobacterium*-mediated genetic transformation in *Arabidopsis thaliana*. Planta **188,** 439–456.

Singh, S. (1993). Role of glutamine synthetase activity in the uptake and metabolism of arginine and proline in cyanobacterium *Anabaena cycadeae.* FEMS Microbiol. Lett. **106,** 335–340.

Szoke, A., Miao, G.-H., Hong, Z., and Verma, D.P.S. (1992). Subcellular location of Δ^1-pyrroline-5-carboxylate reductase in root/nodule and leaf of soybean. Plant Physiol. **99,** 1642–1649.

Temple, S.J., and Sengupta-Gopalan, C. (1997). Manipulating amino acid biosynthesis. In A Molecular Approach to Primary Metabolism in Higher Plants, C.H. Foyer and W.P. Quick, eds (London: Taylor and Francis), pp. 155–177.

Temple, S.J., Bagga, S., and Sengupta-Gopalan, C. (1994). Can glutamine synthetase activity levels be modulated in transgenic plants by the use of recombinant DNA technology? Biochem. Soc. Trans. **22,** 915–920.

Tingey, S.V., Walker, E.L., and Coruzzi, G.M. (1987). Glutamine synthetase genes of pea encode distinct polypeptides that are differentially expressed in leaves, roots and nodules. EMBO J. **6,** 1–9.

Tingey, S.V., Tsai, F.-Y., Edwards, J.W., Walker, E.L., and Coruzzi, G.M. (1988). Chloroplast and cytosolic glutamine synthetase are encoded by homologous genes which are differentially expressed *in vivo*. J. Biol. Chem. **263,** 9651–9657.

Towbin, H., Staehlin, T., and Gordon, J. (1979). Electrophoretic transfer of proteins from polyacrylamide gels to nitrocellulose sheets: Procedure and applications. Proc. Natl. Acad. Sci. USA **76,** 4350–4353.

Vaucheret, H., Kronenberger, J., Lepingle, A., Vilaine, F., Boutin, J.P., and Caboche, M. (1992). Inhibition of tobacco nitrite reductase activity by expression of antisense RNA. Plant J. **2,** 559–569.

Verwoerd, T.C., Dekker, B.N.M., and Hoekema, A. (1989). A small-scale procedure for the rapid isolation of plant RNAs. Nucleic Acids Res. **17,** 2362.

Vézina, L.P., and Langlois, J.R. (1989). Tissue and cellular distribution of glutamine synthetase in roots of pea (*Pisum sativum*) seedlings. Plant Physiol. **90,** 1129–1133.

Vincent, R., Fraisier, V., Chaillou, S., Limami, M.A., Deleens, E., Phillipson, B., Douat, C., Boutin, J.-P., and Hirel, B. (1997). Overexpression of a soybean cytosolic gene encoding glutamine synthetase in shoots of transgenic *Lotus corniculatus* L. plants triggers changes in ammonium assimilation and plant development. Planta **201,** 424–433.

Wallsgrove, R.M., Turner, J.C., Hall, N.P., Kendall, A.C., and Bright, S.W.J. (1987). Barley mutants lacking chloroplast glutamine synthetase: Biochemical and genetic analysis. Plant Physiol. **83,** 155–158.

Watanabe, A., Hamada, K., Yokoi, H., and Watanabe, A. (1994). Biphasic and differential expression of cytosolic glutamine synthetase genes of radish during seed germination and senescence of cotyledons. Plant Mol. Biol. **26,** 1807–1817.

Yamaya, T., and Oaks, A. (1988). Distribution of two isoforms of glutamine synthetase in bundle sheath strands and mesophyll cells of maize leaves. Physiol. Plant. **72,** 23–28.